

Article

Optimization of Desulfurization Process via Choline Phosphotungstate Coupled with Persulfate Using Response Surface Methodology

Yinke Zhang ¹ and Hang Xu ^{2,*}

¹ School of Mathematics and Statistics, Henan University of Science and Technology, Luoyang 471023, China; isoarbj@126.com

² School of Chemistry and Chemical Engineering, Henan University of Science and Technology, Luoyang 471023, China

* Correspondence: xhinbj@126.com

Abstract: Using a simple acid-base neutralization method, a Ch-PW solid catalyst was synthesized by mixing choline hydroxide (ChOH) and phosphotungstic acid (HPW) at a 2:1 molar ratio in an aqueous solution. This catalyst was combined with a 20 wt.% potassium peroxymonosulfate (PMS) solution, using acetonitrile (ACN) as the extraction solvent to create an extraction catalytic oxidative desulfurization system. The optimal desulfurization conditions were determined through response surface methodology, targeting the highest desulfurization rate: 0.99 g of Ch-PW, 1.07 g of PMS, 2.5 g of extraction solvent, at a temperature of 50.48 °C. The predicted desulfurization rate was 90.79%, compared to an experimental rate of 93.64%, with a deviation of 3.04%. A quadratic model correlating the desulfurization rate with the four conditions was developed and validated using ANOVA, which also quantified the impact of each factor on the desulfurization rate: PMS > ACN > Ch-PW > temperature. GC-MS analysis identified the main oxidation product as DBTO₂, and the mechanism of desulfurization in this system was further explored.

Keywords: response surface methodology; desulfurization; choline phosphotungstate; PMS; optimization



Citation: Zhang, Y.; Xu, H. Optimization of Desulfurization Process via Choline Phosphotungstate Coupled with Persulfate Using Response Surface Methodology. *Catalysts* **2024**, *14*, 326. <https://doi.org/10.3390/catal14050326>

Academic Editor: Haralampos N. Miras

Received: 15 April 2024

Revised: 7 May 2024

Accepted: 8 May 2024

Published: 16 May 2024



Copyright: © 2024 by the authors. Licensee MDPI, Basel, Switzerland. This article is an open access article distributed under the terms and conditions of the Creative Commons Attribution (CC BY) license (<https://creativecommons.org/licenses/by/4.0/>).

1. Introduction

The desulfurization of oil products primarily focuses on removing organic sulfur compounds from petroleum products [1]. This crucial process not only reduces sulfur dioxide emissions from burning sulfur-containing fuels, which helps improve air quality and protect the environment, but also safeguards human health. Furthermore, desulfurized fuels enhance the combustion efficiency and extend the life of engines while minimizing wear. Many countries and regions enforce stringent regulations on the sulfur content in petroleum products, compelling refineries to adopt desulfurization practices to comply with environmental standards. Removing sulfur from fuel not only boosts its combustion efficiency but also increases the overall energy system's efficiency. As the focus on environmental protection and energy efficiency intensifies, advancements in desulfurization technologies are spurring research and innovations in this area, particularly in the development of new desulfurization methods and the enhancement of catalysts [2].

Phosphotungstic acid has emerged as a versatile and vital catalyst across a range of applications including the synthesis of fine chemicals, petrochemical processing, water treatment, environmental purification, renewable energy production, organic synthesis, and materials science. Recent advances have particularly highlighted its role in the catalytic oxidative desulfurization of oil products. Wu et al. [3] created spherical PEHA-HPW by simply combining pentamethylene hexamine (PEHA) with phosphotungstic acid (HPW) and used it with hydrogen peroxide to achieve the 100% removal of dibenzothiophene (DBT) within 30 min. Wang et al. [4] developed nanospherical HPW-ZrO₂ catalysts by loading phosphotungstic acid onto zirconium dioxide (ZrO₂), which, when used with hydrogen

peroxide, completely removed DBT, with GC-MS analysis revealing DBTO₂ as the oxidation product. Jangi et al. [5] supported phosphotungstic acid on natural zeolites—clinoptilolite, mordenite, ferrierite, and natrolite—and found that PTA-Ferr exhibited the highest catalytic activity, removing 82.02% of DBT. Xiong et al. [6] formulated phosphotungstic acid ionic liquid materials by dissolving it in octadecyl dimethyl ammonium chloride (OTAC), showing exceptional catalytic performance in the treatment of DBT, 4-MDBT, and 4,6-DMDBT. After 60 min, the desulfurization rates of the three sulfur-containing organic compounds were all close to 100%.

Choline, found naturally, is leveraged in green chemistry due to its environmental friendliness, low volatility, high solubility, affordability, thermal stability, and recyclability. Choline chloride, primarily serving as a hydrogen bond donor, is integral to developing deep eutectic solvents and has emerged as a key player in oil desulfurization [7]. Liu et al. [8] synthesized a choline chloride/2-polyethylene glycol (ChCl/2PEG) deep eutectic solvent that, powered by hydrogen peroxide, removed 99.1% of dibenzothiophene (DBT) in just 3 h. Abbasi et al. [9] combined trichloroacetic acid (TCA) with choline chloride to produce a solvent that, when used with hydrogen peroxide, achieved a 99.6% removal rate for DBT and 91.4% for benzothiophene (BT). Fan et al. [10] formulated a novel deep eutectic solvent by blending choline chloride, benzene sulfonic acid, and ethylene glycol, which removed 100% of DBT, BT, and 4,6-DMDBT within two hours, retaining a 91% desulfurization efficiency even after five cycles. Yue et al. [11] applied molecular dynamics' simulations and free energy perturbation to model the extraction processes of TS/DBT/MDBT with choline chloride-based deep eutectic solvents.

In the process of catalytic oxidative desulfurization, hydrogen peroxide is predominantly used as the oxidant because of its high reactivity and environmentally friendly oxidation byproducts. However, its use is limited by its instability, strong corrosiveness, and high cost. In earlier studies [12–14], our team employed peroxymonosulfate as an alternative oxidant in conjunction with cobalt-based ionic liquid catalysts, achieving highly efficient desulfurization. Peroxymonosulfate stands out for its potent oxidative strength, minimal corrosiveness, affordability, and exceptional stability as a solid salt.

Response surface methodology (RSM) is a statistical approach grounded in experimental design and analysis that seeks the optimal conditions for various processes. It offers numerous benefits including high efficiency, low cost, strong optimization and data analysis capabilities, and wide applicability. RSM is an invaluable tool for researchers and engineers to optimize process parameters, thereby improving production efficiency and product quality while simultaneously reducing costs and enhancing competitiveness. In the realm of desulfurization, RSM has facilitated significant advances: Mahmoudi et al. [15] optimized a magnetically recoverable polyoxometalate-based nanocatalyst with hydrogen peroxide to remove dibenzothiophene (DBT), conducting 20 experiments to pinpoint optimal temperature, oxidant-to-sulfur ratio, and catalyst dosage; Danmaliki et al. [16] optimized the adsorption of DBT using AC-Ni in a flowing phase, identifying ideal conditions for DBT concentration, AC-Ni amount, bed height, flow rate, and contact time; Almashjary et al. [17] formulated a deep eutectic solvent using choline chloride (ChCl) and propionic acid (Pr), employing RSM to fine-tune the desulfurization process and establish the best conditions for the ChCl/Pr ratio, synthesis temperature, extraction temperature, extraction duration, and liquid-to-liquid ratio.

In this research, the desulfurization catalyst Ch-PW was synthesized through an acid-base neutralization reaction between choline hydroxide (ChOH) and phosphotungstic acid (HPW). This catalyst was then integrated with potassium peroxymonosulfate (PMS), a complex salt, to establish a catalytic system for desulfurization. To simulate oil, dibenzothiophene sulfone was dissolved in octane, and acetonitrile (ACN) was employed as the extraction solvent. Utilizing response surface methodology, the optimal process conditions were determined by designing and optimizing the variables of Ch-PW, PMS, ACN, and temperature based on the desulfurization rate.

The main objective of this article is to establish that the coupling of choline phosphotungstate with persulfate constitutes an effective desulfurization system. Subsequently,

using response surface methodology, the optimal conditions for the desulfurization process are rapidly determined, offering a less toxic, more convenient, and highly efficient approach for desulfurization in the oil industry.

2. Results and Discussion

2.1. Experimental Results and Model Selection

Table 1 outlines the desulfurization rates obtained from 29 experimental setups, structured according to the Box–Behnken design. The rates of desulfurization achieved by the Ch-PW/PMS system varied between 29.7% and 93.4%. Notably, the experiments for Run 1, Run 4, Run 14, Run 18, and Run 27 were conducted under the central level conditions (0,0,0,0), achieving desulfurization rates of 90.3%, 88.6%, 93.4%, 91.6%, and 88.4%, respectively. This repetition of experiments under identical conditions serves to assess the random errors inherent in the experimental procedure [18].

Table 1. The Box–Behnken design for the 29 experimental setups alongside their respective results.

Runs	A: Ch-PW /g	B: PMS /g	C: ACN /g	D: Temperature /°C	Removal /%
1	1.00	1.00	2.50	50.00	90.3
2	1.00	0.50	2.50	60.00	35.2
3	1.50	0.50	2.50	50.00	45.6
4	1.00	1.00	2.50	50.00	88.6
5	0.50	0.50	2.50	50.00	47.6
6	1.00	1.50	1.50	50.00	40.6
7	1.00	0.50	3.50	50.00	29.7
8	1.00	1.50	3.50	50.00	73.6
9	1.00	1.00	1.50	40.00	47.6
10	0.50	1.00	3.50	50.00	43.8
11	0.50	1.00	2.50	40.00	52.7
12	1.50	1.00	2.50	40.00	48.5
13	0.50	1.00	1.50	50.00	64.7
14	1.00	1.00	2.50	50.00	93.4
15	1.00	0.50	1.50	50.00	68.7
16	1.50	1.00	1.50	50.00	44.8
17	0.50	1.50	2.50	50.00	52.9
18	1.00	1.00	2.50	50.00	91.6
19	1.00	1.50	2.50	40.00	48.7
20	1.00	1.00	3.50	40.00	60.7
21	1.50	1.00	3.50	50.00	49.8
22	1.00	0.50	2.50	40.00	57.6
23	1.00	1.50	1.50	60.00	63.8
24	1.00	1.50	2.50	60.00	71.2
25	1.50	1.00	2.50	60.00	52.3
26	1.00	1.00	3.50	60.00	49.2
27	1.00	1.00	2.50	50.00	88.4
28	0.50	1.00	2.50	60.00	47.6
29	1.50	1.50	2.50	50.00	52.8

To forecast the experimental conditions that yield the highest desulfurization rates, the Design Expert 8.06 software was utilized to develop a quadratic model. This model delineates the relationship [19] between four experimental factors—the dosage of choline phosphotungstate, potassium peroxy monosulfate solution, acetonitrile addition, and temperature—and the desulfurization rate (removal), as detailed in Equation (1) (a coded factor equation). The selection of the quadratic model, characterized by a Prob>F value less than 0.0001, significantly underscores the model’s robustness and confirms its validity.

$$\text{Removal} = 90.46 - 1.29A + 4.62B - 1.95C + 0.29D + 0.48AB + 6.48AC + 2.22AD + 18.00BC + 11.22BD - 6.92CD - 21.91A^2 - 19.28B^2 - 17.68B^2 - 17.91D^2 \quad (1)$$

Figure 1 depicts the correlation between 29 experimental desulfurization rates and the corresponding 29 predicted rates calculated using Equation (1). The color of the data points in Figure 1 changes from blue to red, representing the change in desulfurization rate from low to high. The alignment of all data points along the coordinate system's diagonal in Figure 1a confirms that the predicted values closely match the experimental results, affirming the appropriateness of the quadratic model. Figure 1b presents the residual plot for these 29 data points, showing a random distribution of residuals. This pattern indicates that the errors are random, lacking any systematic or gross errors. Furthermore, the majority of residuals fall within the -2 to 2 range, underscoring the robustness and credibility of the quadratic model.

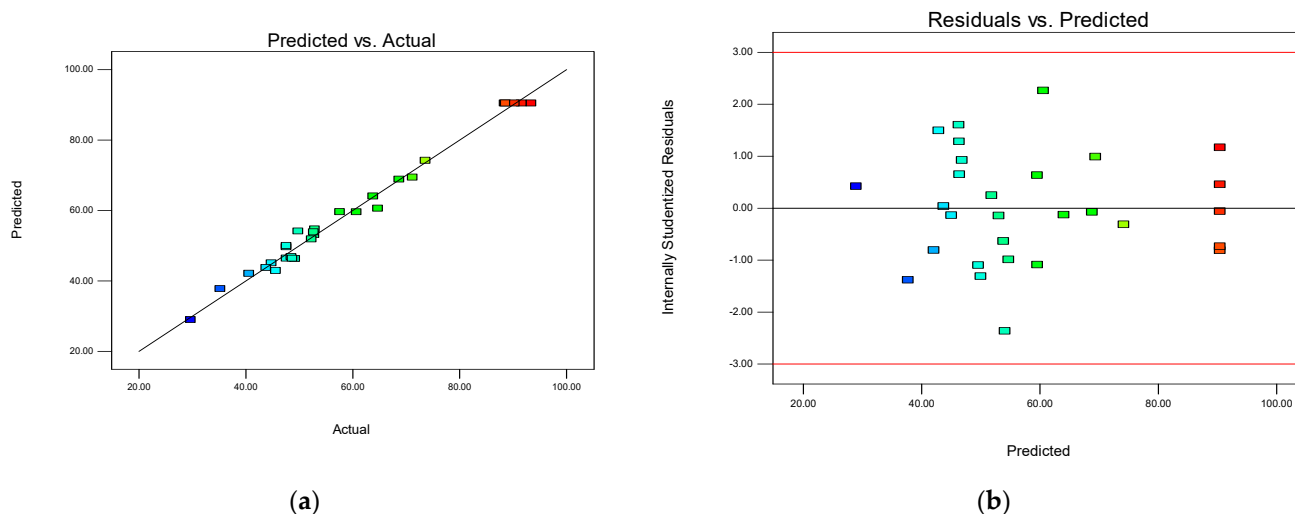


Figure 1. The relationship between predicted vs. actual (a) or residuals vs. predicted (b).

In Figure 1a, the upper right corner displays five parallel red dots, while Figure 1b features five vertical dots on the extreme right. These dots represent the discrepancies between experimental and predicted values, obtained by repeating the central points of 29 Box–Behnken design experiments five times. This repetition is used to ascertain the experimental error at these points, which is essential for evaluating the overall error across all experimental points. Such errors are critical for assessing the model's predictive accuracy and for facilitating further statistical analysis. Since the predicted values remain constant under identical experimental conditions, variations in experimental values lead to the formation of five closely clustered red horizontal dots in Figure 1a, indicating the high precision of the experimental values under consistent conditions. Similarly, the residuals—differences between experimental and predicted values—with constant predicted values result in vertically aligned residual dots as depicted in Figure 1b.

2.2. ANOVA Analysis

Table 2 displays the analysis of variance (ANOVA) derived from the response surface methodology. The model shows a total sum of squares (SS) of 8691.62, with 14 degrees of freedom, a mean square of 620.83, and an F-value of 78.13. The Prob>F value, significantly less than 0.0001, confirms the quadratic model's extreme significance, validating the use of this model to establish the relationships between the four factors and the desulfurization rate (removal). According to the results, the desulfurization rate is predominantly influenced by factor B (PMS), with factor C (ACN) also having a notable impact. In contrast, factors A (Ch-PW) and D (temperature) show a minimal influence. The coefficients for factors A and D in Equation (1)

are considerably smaller than those for B and C, indicating that variations in B and C have a more substantial effect on the desulfurization rate than A and D. The influence hierarchy of the factors on the desulfurization rate is PMS > ACN > Ch-PW > temperature. The minimal influence of the Ch-PW catalyst on the desulfurization rate may be attributed to the chosen levels of the Ch-PW addition being too close to the optimal, resulting in inadequate differentiation.

Table 2. The results of ANOVA analysis.

Source	Sum of Squares	df	Mean Square	F-Value	Prob>F	Significance
Model	8691.62	14	620.83	78.13	<0.0001	**
A-CH-HPW	20.02	1	20.02	2.52	0.1348	No
B-PMS	255.76	1	255.76	32.19	<0.0001	**
C-Acetonitrile	45.63	1	45.63	5.74	0.0311	*
D-Temperature	1.02	1	1.02	0.13	0.7254	No
AB	0.90	1	0.90	0.11	0.7411	No
AC	167.70	1	167.70	21.11	0.0004	**
AD	19.80	1	19.80	2.49	0.1367	No
BC	1296.00	1	1296.00	163.10	<0.0001	**
BD	504.00	1	504.00	63.43	<0.0001	**
CD	191.82	1	191.82	24.14	0.0002	**
A ²	3114.77	1	3114.77	392.00	<0.0001	**
B ²	2410.10	1	2410.10	303.31	<0.0001	**
C ²	2026.61	1	2026.61	255.05	<0.0001	**
D ²	2081.43	1	2081.43	261.95	<0.0001	**
Residual	111.24	14	7.95			
Lack of fit	93.57	10	9.36	2.12	0.2445	No
Pure error	17.67	4	4.42			
Cor total	8802.87	28				
Std. Dev.	2.82		R ²	0.9874		
Mean	58.69		Adj-R ²	0.9747		
C.V.%	4.80		Pred R ²	0.9356		
PRESS	566.58		Adeq precisiior	30.345		

* Significant ($p < 0.05$); ** Extremely significant ($p < 0.01$).

From Table 2, the standard deviation (std. dev.) of 2.82 indicates that the data points closely cluster around the mean, suggesting minimal predictive errors for the model. With a coefficient of variation (C.V.%) of 4.80%, the response variable demonstrates little variability relative to the mean, indicating a low degree of dispersion in the data. An R² value of 0.9874 is exceptionally high, illustrating that the model accounts for nearly all the variability in the data, which signifies an excellent fit. The adjusted R² (Adj-R²) of 0.9747 adjusts for the number of predictors in the model and the degrees of freedom, further validating the model's accuracy. A predictive R² (Pred-R²) of 0.9356 assesses the model's effectiveness in forecasting new datasets, indicating strong predictive performance, though slightly lower than its explanatory capability (i.e., Adj-R²). An adequacy precision (Adeq Precision) of 30.345, which is the ratio of signal to noise, signifies the model's robust ability to distinguish significant effects from random noise, with values above 4 generally indicating a sufficient discriminative capability. Here, a value of 30.345 highlights the model's exceptional predictive discriminative power.

Overall, the ANOVA data demonstrate that the selected quadratic model fits exceptionally well, possesses strong predictive capabilities, minimal errors, and powerful discriminative ability, enabling it to accurately predict response variables.

2.3. Response Surface Analysis

Figure 2 illustrates the response surface plots and contour maps that depict the influence of four factors—catalyst Ch-PW (A), oxidant PMS (B), extraction solvent ACN (C),

and temperature T (D)—on the desulfurization rate. Specifically, Figure 2a displays the interaction between factors A and B, while Figure 2b explores the interaction between factors A and C, and Figure 2c again shows the interaction between factors A and C. From Figure 2a, it is evident that keeping factor B constant, the response (removal) initially rises and then falls as factor A increases from 0.5 to 1.5. Similarly, with factor A constant, factor B exhibits an increase followed by a decrease from 0.5 to 1.5. In Figure 2b,c, with factor A constant, both factors C and D show an initial increase followed by a decrease when increased from 1.5 to 3.5 and from 40 to 60, respectively. These response surface plots demonstrate that optimal values exist for factors A, B, C, and D, confirming that the chosen ranges for these factors are appropriate.

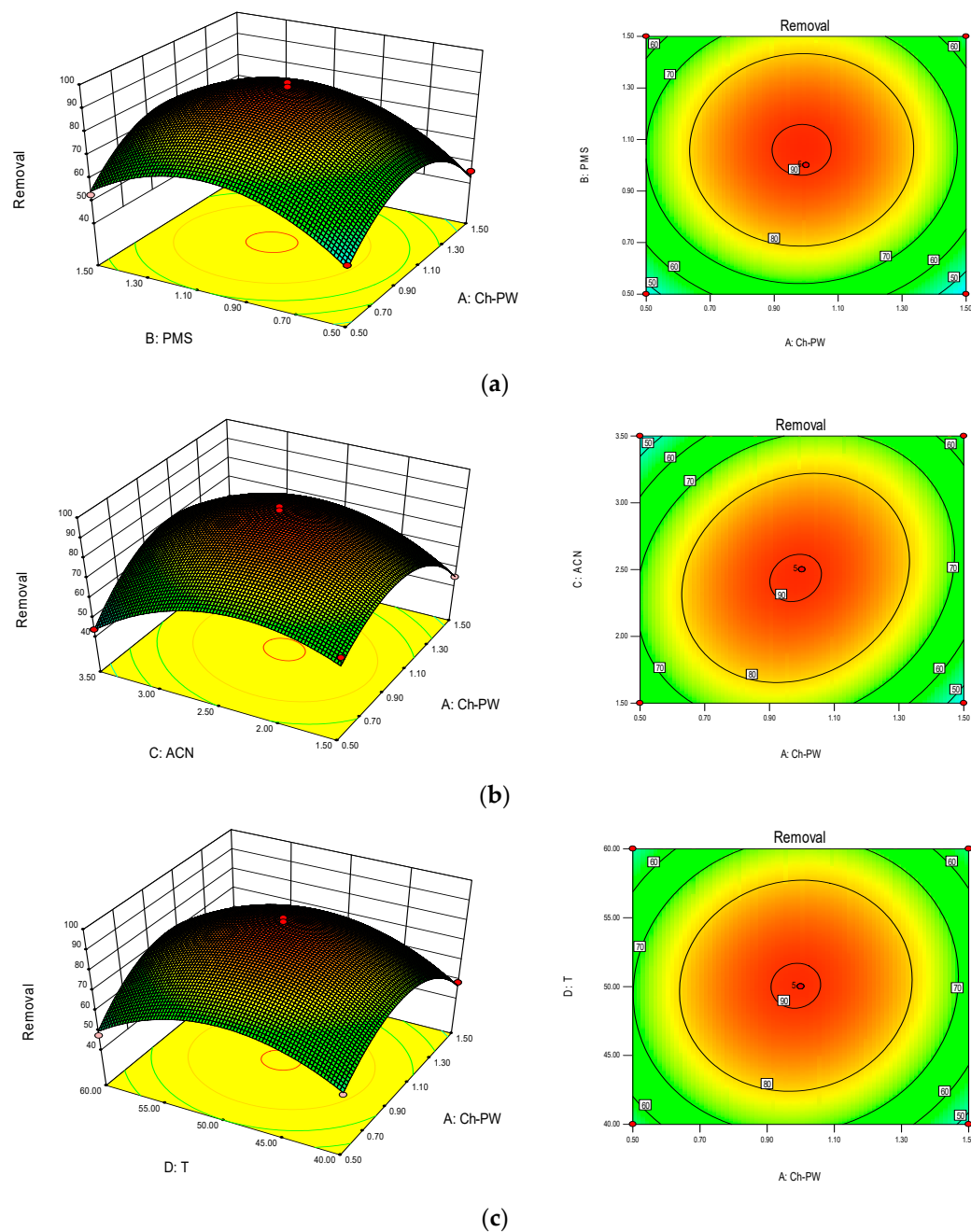


Figure 2. Response surface plots of Ch-PW to PMS (a), ACN (b), and T (c).

From Figure 2a's contour map, the contours formed by factors A and B, as well as A and D, are nearly circular, while those formed by factors A and C deviate from this shape,

forming an ellipse. Circular contours suggest weaker correlations between factors, whereas elliptical contours with an increased curvature indicate stronger correlations. Accordingly, factors A and B, as well as A and D, show relatively weak correlations, while a stronger correlation exists between factors A and C. This aligns with findings from earlier ANOVA analyses.

Reasoning analysis: The desulfurization mechanism hinges on the catalyst Ch-PW, with tungsten atoms serving as electron acceptors. During catalytic oxidation, these facilitate electron transfer to activate the oxidant (B)–peroxymonosulfate-generating sulfate and hydroxyl radicals. These radicals can oxidize dibenzothiophene in the acetonitrile phase, thereby driving desulfurization. Increasing the catalyst enhances the catalytic performance by raising free radical production, thus improving desulfurization rates. However, as the catalyst is solid, it may also consume active radical species, potentially diminishing its effectiveness, indicating an optimal catalyst dosage. Similarly, while more oxidant also increases free radical production, excess ions from the salt can quench these radicals, pointing to an optimal oxidant dosage. Regarding the extraction solvent, its increase can dilute the catalyst and oxidant concentrations, affecting the desulfurization outcomes; optimal concentrations are required for peak efficiency. Finally, while higher temperatures improve reaction rates by reducing solution viscosity, excessive temperatures might increase radical collision and quenching, suggesting an optimal temperature range is essential.

2.4. Optimal Experimental Conditions Determined by Response Surface Methodology

The optimal conditions for the four factors were identified through careful analysis. The response surface methodology yielded the following optimal settings: 0.99 g of catalyst Ch-PW, 1.07 g of PMS, 2.5 g of extraction solvent, and a temperature of 50.48 °C, predicting a desulfurization rate of 90.79%. Experimentally, under these conditions, a desulfurization rate of 93.64% was achieved, with a mere 3.04% deviation between the predicted and actual values, validating the model's predictive accuracy.

Seven experiments were conducted under optimal conditions, each following a consistent cycle: After completing the initial desulfurization, the liquid quickly separated into layers. The upper oil phase (octane phase) was removed, leaving behind the lower extraction phase (ACN phase). Next, 6 g of simulated oil containing 500 ppm sulfur and 1.07 g of PMS (20 wt.%) was added. Both the temperature and reaction time were maintained constant for the subsequent desulfurization trial, and the corresponding desulfurization rate was recorded. This procedure was repeated through seven trials in total. As depicted in Figure 3, the desulfurization rate stayed above 90% for the first five trials. However, it dropped to 85% after the sixth trial and further decreased to 80% after the seventh. The desulfurization system demonstrated robust recyclability characteristics.

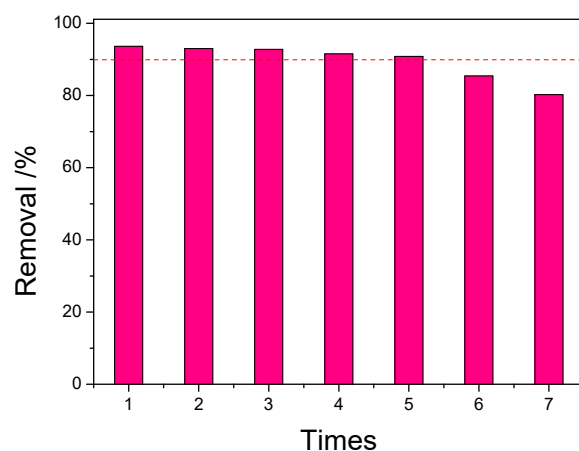


Figure 3. The recycling performance of desulfurization system.

During the cyclic experimental process, the upper oil phase is removed after each experiment, and fresh oil and oxidant are introduced for the next trial. Over time, the contamination on the surface of Ch-PW decreases its activity. Furthermore, the accumulation of sulfate ions, oxidation byproducts in the acetonitrile phase, is not removed throughout the cycles. This leads to a significant impairment of the desulfurization activity, ultimately causing deactivation.

2.5. Analysis of Desulfurization Products and Mechanism

To elucidate the desulfurization mechanism of Ch-PW coupled with PMS, GC-MS analysis was conducted on the desulfurization products within the acetonitrile phase, as depicted in Figure 4a,b. The GC trace in Figure 4a reveals two distinct peaks, one high and one low. The lower peak, with a retention time of 16.3 min, was identified as DBT, while the higher peak at 20.65 min was determined to be DBTO₂, as illustrated in Figure 4b. This analysis confirms that DBTO₂ is the principal oxidation product of DBT.

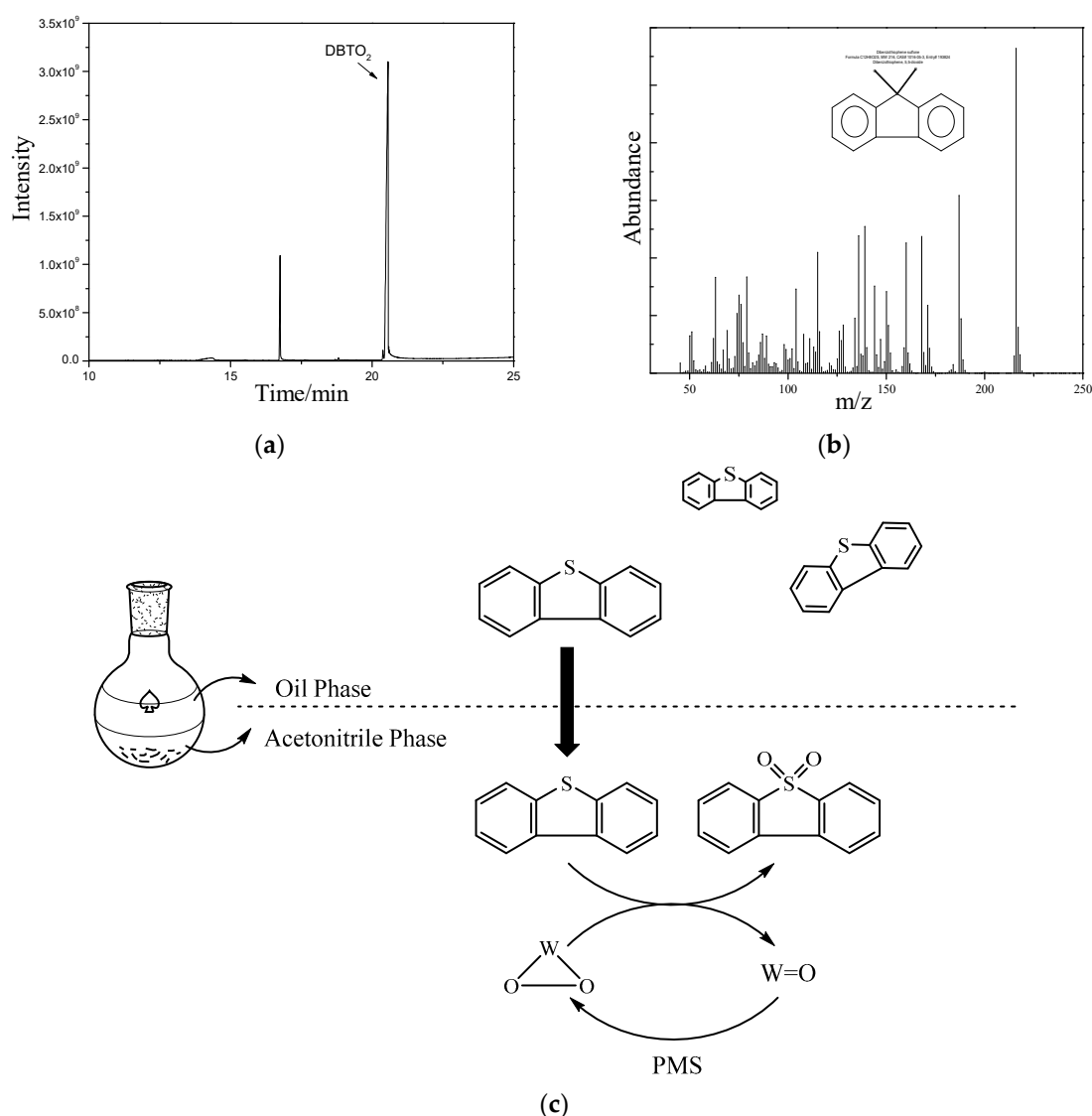


Figure 4. GC-MS in acetonitrile phase and mechanism of desulfurization: (a) GC; (b) MS; (c) desulfurization mechanism.

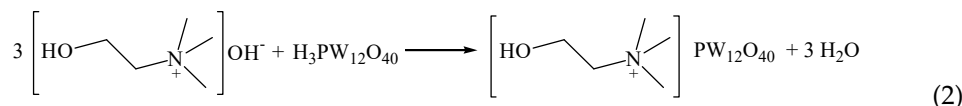
The desulfurization mechanism, inferred from the GC-MS findings, is outlined in Figure 4c. Initially, acetonitrile, serving as the extraction solvent, extracts dibenzothiophene from the simulated oil into the acetonitrile phase. Subsequently, dibenzothiophene is

oxidized by the combined action of the oxidant PMS and catalyst Ch-PW in the acetonitrile phase. Ch-PW interacts with PMS to generate $\{PO_4[W(O)(O_2)_2]_4\}^{3-}$ anionic species, with the tungsten-oxygen active centers exhibiting potent oxidizing capabilities, swiftly converting thiophenic compounds and their derivatives into sulfoxides or sulfones. Owing to acetonitrile's presence, dibenzothiophene continuously extracted into the acetonitrile phase is transformed into a sulfone, increasing its polarity and thus retaining it within the acetonitrile phase. Throughout this process, Ch-PW remains catalytically active, facilitated by the activation of PMS, until the consumption of PMS is complete.

3. Experimental Section

3.1. Preparation of Choline Phosphotungstate (Ch-PW) [20]

Weigh 7.2 g of phosphotungstic acid (HPW) and dissolve in 10 mL of deionized water while stirring. Separately, dissolve 1.86 g of choline in another 10 mL of deionized water and stir. Gradually add this choline solution to the phosphotungstic acid solution, which results in the immediate formation of a white precipitate. Continue stirring the mixture at room temperature for an additional 5 h after the addition is complete. Subsequently, filter the mixture and rinse the precipitate thoroughly with deionized water several times. Dry the precipitate at 70 °C for 48 h to obtain the white solid of choline phosphotungstate, as depicted in reaction Formula (2).



3.2. Catalytic Oxidative Desulfurization Process

Dibenzothiophene (DBT) was dissolved in n-octane to formulate a simulated oil, which was adjusted to a sulfur content of 500 ppm. To this, 6 g of simulated oil, a specified quantity of Ch-PW, 20 wt.% potassium peroxymonosulfate complex salt (PMS), and acetonitrile (ACN) were added. The mixture was continuously stirred at a regulated temperature until the desulfurization reaction was completed. Throughout the reaction, samples of the upper oil layer were periodically drawn and analyzed using a spectrophotometer. The characteristic absorption peak of DBT at 312 nm was determined using UV-visible spectrophotometry, establishing a relationship between absorbance (A) and sulfur content (S) as follows: $A = 53.00591S - 0.00484$ ($R^2 = 0.9992$). The desulfurization rate (R) was calculated according to Formula (3), where S_0 denotes the initial sulfur concentration of 500 ppm.

$$R = (S_0 - S) \times 100\% / S_0 \quad (3)$$

3.3. Design of Desulfurization Process Using Response Surface Methodology

A four-factor, three-level Box–Behnken design (BBD) was employed to optimize the desulfurization process, utilizing Design Expert 8.06 software [21]. The variables considered included the dosage of choline phosphotungstate (Ch-PW, g), potassium peroxymonosulfate solution (PMS, g), acetonitrile (ACN, g), and temperature (T, °C), denoted as A, B, C, and D, respectively. Each variable was tested at three levels, as detailed in Table 3.

Table 3. Box–Behnken design, outlining the factors and their coded levels.

Factors	Unit	Level		
		−1	0	1
A: Ch-PW	g	0.5	1	1.5
B: PMS	g	0.5	1	1.5
C: ACN	g	1.5	2.5	3.5
D: T	°C	40	50	60

As can be seen from Table 3, the selection range for Ch-PW is 0.5 to 1.5 g, the selection range for the PMS solution is also 0.5 to 1.5 g, the selection range for ACN is 1.5 to 3.5 g, and the selection range for T is 40 to 60 °C. To choose a relatively reasonable range, preliminary experiments were conducted. The selection of ACN is because ACN is immiscible with octane and has good solubility for DBT. ACN can extract some of the DBT in the octane phase, which is beneficial for subsequent catalytic oxidation.

4. Conclusions

Choline hydroxide (ChOH) and phosphotungstic acid (HPW) were combined in a 3:1 molar ratio through a straightforward acid-base neutralization reaction to synthesize the Ch-PW catalyst. This catalyst was integrated with a 20 wt.% potassium peroxymonosulfate complex salt (PMS) solution and acetonitrile (ACN) as the extraction solvent, forming an extraction catalytic oxidative desulfurization system. This system was employed to remove dibenzothiophene (DBT) dissolved in octane, simulating a sulfur-containing oil environment. Optimal conditions for achieving the highest desulfurization rate, as optimized through response surface methodology, included 0.99 g of Ch-PW, 1.07 g of PMS, 2.5 g of ACN, and a temperature of 50.48 °C. Under these conditions, the predicted desulfurization rate was 90.79%, with an actual rate of 93.64% observed, resulting in a minor deviation of 3.04%. A model relating desulfurization rate to these conditions was established and validated using ANOVA, which also quantified the influence of the factors on the desulfurization rate: PMS > ACN > Ch-PW > temperature. The desulfurization products were analyzed by GC-MS, which identified DBTO₂ as the primary oxidation product. Additionally, the mechanism underlying the system's desulfurization was thoroughly investigated.

Author Contributions: Conceptualization, H.X.; methodology, Y.Z.; software, Y.Z.; validation, Y.Z. and H.X.; formal analysis, H.X.; investigation, H.X.; resources, H.X.; data curation, Y.Z. and H.X.; writing—original draft preparation, Y.Z.; writing—review and editing, H.X.; visualization, Y.Z.; supervision, H.X.; project administration, H.X.; funding acquisition, H.X. All authors have read and agreed to the published version of the manuscript.

Funding: This study was supported by the Nature Science Foundation of Henan Province (No. 202300410155).

Data Availability Statement: The data presented in this study are available on request from the corresponding author.

Conflicts of Interest: The authors declare no conflicts of interest.

References

1. Karamzadeh, M.; Movahedirad, S.; Sobati, M.A. Desulfurization of oxidized diesel fuel in a spiral micro-channel contactor under ultrasound irradiation. *J. Environ. Chem. Eng.* **2023**, *11*, 109780. [[CrossRef](#)]
2. Salem, H.M.; Abdelrahman, A.A. Sono-catalytic oxidative desulfurization of fuels using Fe₆W₁₈O₇₀@ZrFe₂O₅. *J. Alloys Compd.* **2023**, *956*, 170275. [[CrossRef](#)]
3. Wu, C.F.; Chen, C.S.; Qi, Z.Y.; Chen, J.; Wang, Q.L.; Ye, C.S.; Qiu, T. Facile synthesis of efficient pentaethylenehexamine-phosphotungstic acid heterogeneous catalysts for oxidative desulfurization. *Chin. J. Chem. Eng.* **2023**, *63*, 140–147. [[CrossRef](#)]
4. Wang, P.; Gan, M.X.; Deng, P.H.; Xu, Y.F.; Hou, Y. Phosphotungstic acid-supported zirconia mesoporous material for deep and fast oxidative desulfurization. *Inorg. Chem. Commun.* **2021**, *133*, 108922. [[CrossRef](#)]
5. Jangi, F.; Rahemi, N.; Allahyari, S. Oxidative desulfurization using nanocomposites of heterogeneous phosphotungstic acid over natural zeolites; optimization by central-composite design. *Pet. Sci. Technol.* **2023**, *41*, 104–122. [[CrossRef](#)]
6. Xiong, J.; Huang, H.X.; Zhang, M.; Song, P.; Li, H.P.; Di, J. Incorporating carbon quantum dots into phosphotungstic acid ionic liquid materials for enhanced catalytic oxidative desulfurization. *Fuel* **2024**, *365*, 131168. [[CrossRef](#)]
7. Jiang, W.; Dong, L.; Liu, W.; Guo, T.; Li, H.P.; Yin, S.; Zhu, W.S.; Li, H.M. Biodegradable choline-like deep eutectic solvents for extractive desulfurization of fuel. *Chem. Eng. Process. -Process Intensif.* **2017**, *115*, 34–38. [[CrossRef](#)]
8. Liu, W.; Jiang, W.; Zhu, W.Q.; Zhu, W.S.; Li, H.P.; Guo, T.; Zhu, W.H.; Li, H.M. Oxidative desulfurization of fuels promoted by choline chloride-based deep eutectic solvents. *J. Mol. Catal. A Chem.* **2016**, *424*, 261–268. [[CrossRef](#)]
9. Abbasi, A.; Feyzi, F. Oxidation/extraction desulfurization with carboxylic acid-based deep eutectic solvents. *Pet. Sci. Technol.* **2022**, *40*, 751–766. [[CrossRef](#)]

10. Fan, K.; Yang, B.; Yu, S.S.; Yang, R.G.; Zhang, L.F.; Chi, W.J.; Yin, M.H.; Wu, H.D.; Guo, J. Ternary choline chloride/benzene sulfonic acid/ethylene glycol deep eutectic solvents for oxidative desulfurization at room temperature. *RSC Adv.* **2023**, *12*, 25888–25894. [[CrossRef](#)] [[PubMed](#)]
11. Yue, K.; Acevedo, O. Uncovering the Critical Factors that Enable Extractive Desulfurization of Fuels in Ionic Liquids and Deep Eutectic Solvents from Simulations. *J. Phys. Chem. B* **2023**, *127*, 6354–6373. [[CrossRef](#)]
12. Xu, H.; Zhang, D.D.; Wu, F.M.; Wei, X.F.; Zhang, J. Deep desulfurization of fuels with cobalt chloride-choline chloride/polyethylene glycol metal deep eutectic solvents. *Fuel* **2018**, *225*, 104–110. [[CrossRef](#)]
13. Zhang, Y.K.; Li, L.; Shang, Z.H.; Xu, H. Application of a Response Surface Method for the Optimization of the Hydrothermal Synthesis of Magnetic NiCo₂O₄ Desulfurization Catalytic Powders. *Catalysts* **2023**, *13*, 1119. [[CrossRef](#)]
14. Zhang, Y.K.; Xu, H.; Jia, M.F.; Liu, Z.; Qu, D.Q. Optimization of Deep Oxidative Desulfurization Process Using Ionic Liquid and Potassium Monopersulfate. *J. Chem.* **2018**, *2018*, 6495826. [[CrossRef](#)]
15. Mahmoudi, V.; Kermani, A.M.; Ghahramaninezhad, M.; Ahmadpour, A. Oxidative desulfurization of dibenzothiophene by magnetically recoverable polyoxometalate-based nanocatalyst: Optimization by response surface methodology. *Mol. Catal.* **2021**, *509*, 111611. [[CrossRef](#)]
16. Danmaliki, G.I.; Saleh, T.A.; Shamsuddeen, A.A. Response surface methodology optimization of adsorptive desulfurization on nickel/activated carbon. *Chem. Eng. J.* **2017**, *313*, 993–1003. [[CrossRef](#)]
17. Almashjary, K.H.; Khalid, M.; Dharaskar, S.; Jagadish, P.; Walvekar, R.; Gupta, T.C.S.M. Optimisation of extractive desulfurization using Choline Chloride-based deep eutectic solvents. *Fuel* **2018**, *234*, 1388–1400. [[CrossRef](#)]
18. Prabha, B.; Ramesh, D.; Sriramajayam, S.; Uma, D. Optimization of Pyrolysis Process Parameters for Fuel Oil Production from the Thermal Recycling of Waste Polypropylene Grocery Bags Using the Box-Behnken Design. *Recycling* **2024**, *9*, 15. [[CrossRef](#)]
19. Ali, H.; Yasir, M.; Ngwabebhoh, F.A.; Sopik, T.; Zandraa, O.; Sevcik, J.; Masar, M.; Machovsky, M.; Kuritka, I. Boosting photocatalytic degradation of estrone hormone by silica-supported g-C₃N₄/WO₃ using response surface methodology coupled with Box-Behnken design. *J. Photochem. Photobiol. A Chem.* **2023**, *441*, 114733. [[CrossRef](#)]
20. Zeng, X.Y.; Xiao, X.Y.; Chen, J.Y.; Wang, H.L. Electron-hole interactions in choline-phosphotungstic acid boosting molecular oxygen activation for fuel desulfurization. *Appl. Catal. B Environ.* **2019**, *248*, 573–586. [[CrossRef](#)]
21. Wyantuti, S.; Fadhilatunnisa, B.; Fauzia, R.P.; Jia, Q.; Rahmani, A.A.; Bahti, H.H. Response surface methodology box-behnken design to optimise the hydrothermal synthesis of gadolinium nanoparticles. *Chin. J. Anal. Chem.* **2023**, *51*, 100316. [[CrossRef](#)]

Disclaimer/Publisher's Note: The statements, opinions and data contained in all publications are solely those of the individual author(s) and contributor(s) and not of MDPI and/or the editor(s). MDPI and/or the editor(s) disclaim responsibility for any injury to people or property resulting from any ideas, methods, instructions or products referred to in the content.